

A unified force control approach to autonomous underwater manipulation

Yong Cui and Nilanjan Sarkar

Department of Mechanical Engineering, Vanderbilt University, Nashville, TN 37235 (USA)

(Received in Final Form: September 12, 2000)

SUMMARY

A unified force control scheme for an autonomous underwater robotic system is proposed in this paper. This robotic system is composed of a six degree-of-freedom autonomous underwater vehicle (AUV) and a robotic arm that is mounted on the AUV. A unified force control approach, which combines impedance control with hybrid position/force control by means of fuzzy switching to perform autonomous underwater manipulation, is presented in this paper. This controller requires a dynamic model of the underwater vehicle-manipulator system. However, it does not require any model of the environment and therefore will have the potential to be useful in underwater tasks where the environment is generally unknown. The proposed approach combines the advantages of impedance control with hybrid control so that both smooth contact transition and force trajectory tracking can be achieved. In the absence of any functional autonomous underwater vehicle-manipulator system that can be used to verify the proposed controller, extensive computer simulations are performed and the results are presented in the paper.

KEYWORDS: Underwater robotics; Force control; Underwater vehicle-manipulator systems

1. INTRODUCTION

Ocean covers a large part of the earth, most of which still remains unexplored. Underwater robotic vehicles (URVs), which include both remotely operated vehicles (ROVs) and autonomous underwater vehicles (AUVs), are effective tools to help people explore this unfamiliar world. When robotic manipulators are mounted on the ROVs and the AUVs, the combined system is usually called *Underwater Vehicle-Manipulator Systems* (UVMS). The UVMS are more effective when interaction with the environment is required. These systems have been used for inspection, drilling, mine countermeasures, surveying, underwater cable burial, inspection of power plant conduits and so on.¹ Currently the master-slave configuration of underwater manipulation system is widely used. This type of configuration has a few disadvantages, such as low accuracy of trajectory tracking, difficulty to realize accurate force control, high operational cost, time delay in the man-machine control loop in an unstructured environment and operator's fatigue. To overcome these deficiencies, an unmanned *autonomous* vehicle-manipulator control system that can simultaneously

control the position of the end-effector and the force applied to the environment, would be useful. Thus UVMS in the context of this paper will imply autonomous UVMS.

The model-based free space motion control of the UVMS has been studied and several control schemes have been developed. The dynamic interactions between the vehicle and the manipulator have been analyzed and included into the system model.^{2,3} A challenging part of this type of control is to obtain an accurate model of the hydrodynamic reactions. Since the UVMS is a nonlinear, time varying system and the hydrodynamic effects cannot be modeled accurately, adaptive or learning control schemes have been proposed.⁴ The kinematic redundancy of a UVMS has also been utilized to improve the performance of motion control, such as avoiding singularities, obstacles, improving dexterity, and power optimization.⁵

Most underwater manipulation tasks, such as underwater pipeline or weld inspection and mating of underwater connector or socket, require physical contact between the manipulator and the underwater environment. Thus force control is necessary for a UVMS to effectively function in an underwater environment. Although many force control schemes have been developed for earth-fixed manipulators and space robots, these control methods cannot be used directly in UVMS because of the uncertainties of the system dynamic model and the unstructured nature of the underwater environment. There are several difficulties that are associated with the force control of UVMS and must be solved before we can design an effective force control algorithm. Some of these problems are: (1) It is difficult to obtain accurate models for the manipulator, vehicle and the underwater environment. Especially the hydrodynamic model is not accurate. (2) The UVMS is a highly nonlinear, coupled, and MIMO (multi-input and multi-output) system. It is difficult to find an effective position and force control scheme for both unconstrained and constrained motion control of the UVMS. (3) It is difficult to model the dynamic interactions between the manipulator and the underwater vehicle. (4) The UVMS is a kinematically redundant system where the degrees-of-freedom (DOF) of the underwater vehicle are less accurately controlled than that of the manipulator.⁵ It is problematic to negotiate the geometric uncertainty of the underwater environment.

There are only a few research publications that deal with the force control of a UVMS. In reference [6], a hybrid position/force control scheme was developed and tested on a TA9 hydraulic manipulator mounted on an underwater



vehicle. However, the dynamic coupling between the manipulator and the underwater vehicle was not considered in the system model. Kajita and Kosuge⁷ presented a method that utilized the restoring force generated by the thrusters to compensate the contact force at the endpoint of the manipulator mounted on a floating vehicle. Another position/force control method was introduced in reference [8], which used a force control loop inside a position control loop to compensate for the position errors caused by the torque produced by the arm. Both these methods were limited to controlling the vehicle separately instead of controlling the system as a whole. In reference [9], the difficulties of force control of UVMS are presented and an external force control scheme is introduced.

The objective of the present paper is to propose a unified force control approach that can be effective for both unconstrained and constrained motion of the UVMS. The idea is to combine two separate control schemes, impedance control and hybrid position/force control, in such a way that the UVMS can both negotiate a contact and then follow a desired force trajectory without an accurate knowledge of the environment. This paper advances our preliminary work¹⁰ on the impedance control of UVMS. The rest of the paper is organized as follows. In Section 2, we discuss the background and philosophy of our proposed unified force control scheme. We then present a dynamic model of a UVMS including model for thruster dynamics in the following section. This dynamic model is utilized in designing the unified controller in Section 4. We present results from computer simulations in Section 5. Finally, in Section 6 we summarize our contributions and discuss possible future work.

2. UNIFIED FORCE CONTROL FOR A UVMS – BACKGROUND AND RATIONALE

Many underwater tasks require contact between the end-effector of the manipulator of the UVMS and the underwater environment, and then application of certain contact force on the environment. Thus the UVMS must first move to the specific location in its environment and then apply specific forces. There are three distinct phases in this process: an unconstrained motion, a transient contact and a constrained motion. The force control strategies must perform two specific functions. First, they must provide impact control and be stable during the transient phase of the impact with the environment. Second, they must provide force trajectory tracking capability.

There are currently no three-phase control strategies available for a UVMS. There are, however, several control strategies that can be used to realize this three-phase control requirement for land-based robotic systems. One of these strategies is called hybrid impedance control, which uses duality principle to determine which kind of control can be used for a particular degrees-of-freedom based on the character of the environment.¹¹ In reference [12], two impedance control schemes, direct adaptive control and indirect adaptive control, are developed for force tracking. The first scheme uses the force tracking-error to generate the reference position of the impedance controller. In the second one, the reference position is computed based on the

environmental parameter estimation. Shibata et al.¹³ developed a unified approach based on the second scheme of reference [12] to realize the force tracking. Position and force are both controlled along the same direction and fuzzy logic was employed to switch from position to force control and vice versa. The force tracking is obtained by estimating the parameters of the environment and then computing the reference position based on this estimation. However, for underwater tasks, it is difficult to obtain the parameters of the underwater environment and then to estimate these parameters by fast sampling rate. Additionally, for UVMS, the model that needs to be used for force control is usually derived in the vehicle-fixed frame and may require a transformation from that frame to an inertial frame before a force controller can be designed.

We propose a new unified force control approach that can both achieve a stable contact and track a desired force trajectory *without* the knowledge of the underwater environment. This method combines the impedance control with the hybrid position/force control by means of fuzzy switching. First, we describe each component of the proposed control scheme and then present the structure of the proposed unified controller.

Robot Force control is an active research field and many control schemes have been developed in the past few decades.^{14,15} Among these schemes, hybrid position/force control¹⁶ decomposes the task space into two orthogonal subspaces, position-subspace and force-subspace, by a compliance selection matrix S . Hybrid position/force control can be expressed as

$$T_i = \sum_{j=1}^N \left\{ \Gamma_{ij} \left[S_j \Delta f_j \right] + \Psi_{ij} \left[(1 - S_j) \Delta x_j \right] \right\} \quad (1)$$

where N : number of DOF; T_i : torque applied by the i -th actuator; Δf_j : force error at the j -th DOF; Δx_j : position error at the j -th DOF; Γ_{ij} : force compensation function (force control law); Ψ_{ij} : position compensation function (position control law); S_j : component of the compliance selection vector, which can be selected either 1 or 0 to determine the direction that must be force controlled or position controlled. Then each subspace is controlled separately using a position or a force controller. Generally, explicit force control schemes are used in the force control sub-loop, so that the force tracking can be achieved.

A UVMS fundamentally requires the manipulator be mechanically coupled with the underwater environment to keep it stable during the transient phase. A stable contact is important for UVMS, because excessive contact force will damage the arm or the object and will consume more energy to stabilize the vibration. It is difficult to meet this requirement by hybrid position/force control, because it neglects the mechanical work between the system and the environment. The aim of impedance control¹⁷ is to control mechanical impedance of the manipulator and the environment instead of controlling position or force alone. Additionally, impedance control does not require the control switching, which is needed in hybrid control from uncon-

strained motion to constrained motion. The drawback of this scheme, however, is that it is difficult to obtain force tracking without the knowledge of the contacting environment. The underwater environment is generally unknown and thus force tracking is not possible by using impedance control alone.

Thus it is clear from the above discussion that hybrid control with explicit force control scheme in force control subsystem can track a desired force trajectory. However, hybrid control needs to switch from unconstrained motion control to constrained motion control during the transient phase. This switching usually generates a large force surge and can make the system unstable. The advantage of the impedance control, on the other hand, is that it can control the dynamic characteristics of the system and achieves a smooth impact with the environment.¹² In the proposed unified force control scheme, impedance control is used for the impact phase to achieve a ‘soft’ contact. Once the contact is established in a stable manner, hybrid control is used to allow the end-effector to follow a desired force trajectory. In the transient phase, a fuzzy switch is employed to combine the output of the impedance control with that of the hybrid control into one control output according to the force and velocity signals. If we design the controller in the task space, the control output, F_c can be expressed as

$$F_c = F_{IP}W + F_H(1 - W) \tag{2}$$

where F_{IP} is the output of the impedance sub-controller and F_H is the output of the hybrid position/force sub-controller. W is the weight set by fuzzy switching law. A simplified block diagram of this controller is shown in Fig. 1.

3. DYNAMICS OF A UVMS

The dynamics of a UVMS is highly coupled, nonlinear and time-varying. We develop the dynamic equations of motion of such a system by using a *Quasi-Lagrange* formulation, the details of which can be found in references [5] and [18]. We provide the fundamental structure of the dynamic equations without going into the derivation. This dynamic model is used to design the proposed unified force controller in the next section. This formulation is attractive because it is similar to the widely used standard Lagrange formulation but it generates the equations of motion in the body-fixed, non-inertial reference frame, which is useful for a UVMS.

3.1 Quasi-Lagrange Formulation

We briefly describe the forms of equations of motion when they are derived using a *Quasi-Lagrange* formulation. Consider an n DOF dynamic system. The fundamental form of the Lagrange equation of motion in the matrix form is

$$\frac{d}{dt} \left(\frac{\partial T}{\partial \dot{q}} \right) - \left(\frac{\partial T}{\partial q} \right) = Q \tag{3}$$

where T =kinetic energy of the system in the inertial frame, q =the vector of generalized coordinates, \dot{q} =the vector of first time derivative of the generalized coordinates, and Q =the vector of generalized forces applied to the system. Now consider the velocity vector when expressed in a body-fixed frame, $w = [w_1, w_2, \dots, w_n]^T$. The difference between \dot{q}_j and w_i is that the former can be integrated with respect to time to obtain the displacements q_j , whereas w_i may not be integrated to obtain displacements. It is customary to refer

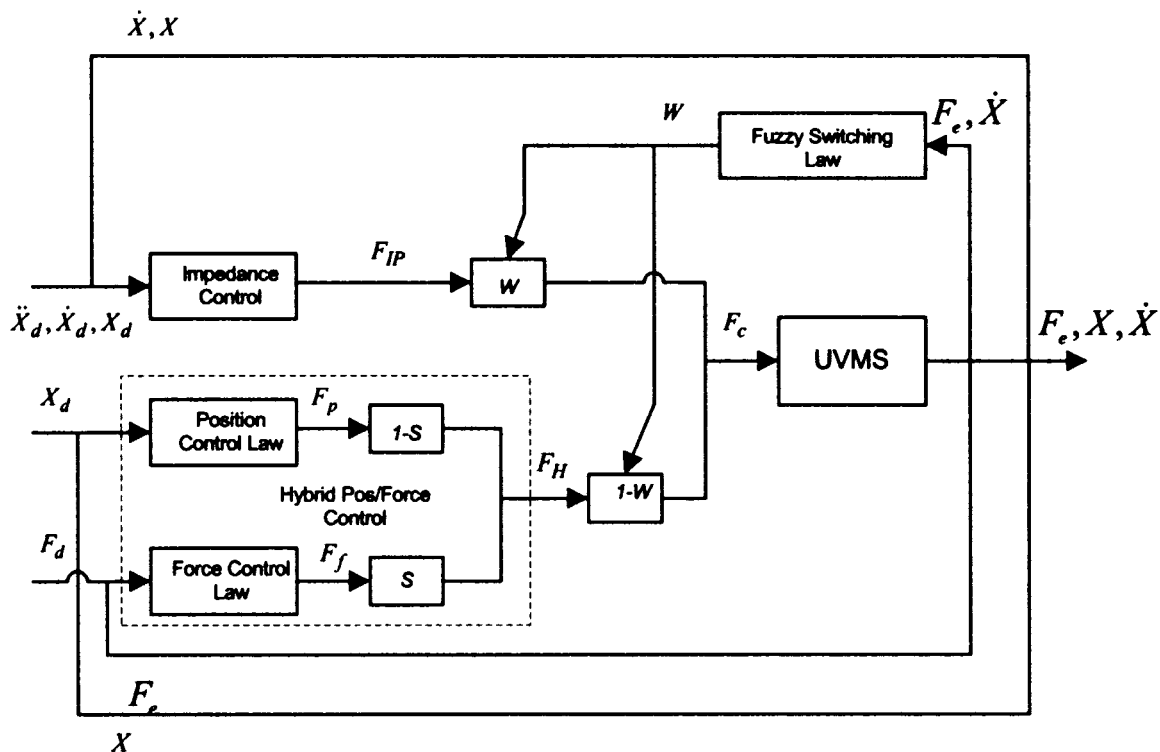


Fig. 1. The unified force control scheme.

w_i as *quasi-velocities* or the derivatives of quasi-coordinates.¹⁸

The \dot{q}_j and w_i are related as follows:

$$\dot{q} = Bw \tag{4}$$

where B is an $n \times n$ transformation matrix.

Using the above relation, Equation (3) can be represented in the following form (A detailed derivation is omitted here for brevity and can be found in reference [5]):

$$\frac{d}{dt} \left(\frac{\partial \bar{T}}{\partial w} \right) + B^T \gamma \frac{\partial \bar{T}}{\partial w} - B^T \frac{\partial \bar{T}}{\partial q} = \tau \tag{5}$$

where \bar{T} is the kinetic energy expressed as a function of w .

This is referred to as *Quasi Lagrange equations*, where

$$\gamma = \left[w^T B^T \frac{\partial A}{\partial q} \right] - \left[w^T B^T \left[\frac{\partial A}{\partial q} \right] \right] \tag{6}$$

and $BA^T = I$, $\frac{\partial A}{\partial q}$ is an $n \times 1$ column vector and $\left[\frac{\partial A}{\partial q} \right]$ is an $n \times n$ square matrix.

$$\tau = B^T Q \tag{7}$$

3.2 Dynamic equations of motion of a UVMS

The dynamic equations of motion of a UVMS can be expressed as follows:

$$M_b(q_m)\dot{w} + C_b(q_m, w)w + D_b(q_m, w)w + G_b(q) = \tau_b \tag{8}$$

where the subscript ‘ b ’ denotes the corresponding parameters in the body-fixed frame of the UVMS $M_b(q_m)$ is the $(6+n) \times (6+n)$ inertia matrix which includes both the rigid body and the added mass inertia, $C_b(q_m, w)$ is the $(6+n) \times 1$ vector of centrifugal and Coriolis forces/moments including terms due to both rigid body and added mass, $D_b(q_m, w)$ is the $(6+n) \times 1$ vector of drag forces/moments, $G_b(q)$ is the $(6+n) \times 1$ vector of gravity and buoyancy forces/moments and τ_b is the $(6+n) \times 1$ vector of forces/moments acting on the UVMS. $q = [q_v, q_m]^T$, where $q_v = [q_1, \dots, q_6]^T$, and $q_m = [q_7, \dots, q_{6+n}]^T$ are the generalized coordinates. q_1, q_2 and

q_3 are the linear displacements of the vehicle along the X, Y and Z axes, respectively, expressed in the earth-fixed frame, XYZ, and q_4, q_5 and q_6 are the angular (roll, pitch, and yaw) rotations of the vehicle about the X, Y and Z axes, respectively, expressed in the earth-fixed frame, XYZ (Fig. 2). q_7, q_8, \dots, q_{6+n} are the displacements of joint 1, joint 2, ..., joint n of the manipulator in link attached frames. The quasi velocity vector $w = [w_1, \dots, w_{6+n}]^T$, where w_1, w_2 and w_3 are the linear velocities (surge, sway, and heave) of the vehicle along the $X_v, Y_v,$ and Z_v axes respectively, and expressed in the body-fixed frame, and w_4, w_5 and w_6 are the angular velocities (roll, pitch and yaw) of the vehicle about the $X_v, Y_v,$ and Z_v axes respectively, expressed in the body-fixed frame. w_7, w_8, \dots, w_{6+n} are the angular velocities of manipulator joint 1, joint 2, ..., joint n . A detailed derivation of Equation (8) is given in reference [5].

The matrix B in Equation (4) is given by:

$$B(q) = \begin{bmatrix} B_{1_{6 \times 6}} & O_{6 \times n} \\ O_{n \times 6} & B_{2_{n \times n}} \end{bmatrix}, B_1 = \begin{bmatrix} J_1 & O \\ O & J_2 \end{bmatrix}, B_2 = [I]$$

where the linear velocity transformation J_1 and the angular velocity transformation J_2 between the inertial and the vehicle-fixed frame are:

$$J_1 = \begin{bmatrix} C_5 C_6 & -S_6 C_4 + S_4 S_5 C_6 & S_4 S_6 + S_5 C_4 C_6 \\ S_6 C_5 & C_4 C_6 + S_4 S_5 S_6 & -S_4 C_6 + S_5 S_6 C_4 \\ -S_5 & S_4 C_5 & C_4 C_5 \end{bmatrix}$$

$$J_2 = \begin{bmatrix} 1 & S_4 T_5 & C_4 T_5 \\ 0 & C_4 & -S_4 \\ 0 & S_4 / C_5 & C_4 / C_5 \end{bmatrix}$$

Here S_i, C_i and T_i represent $\sin(q_i), \cos(q_i)$ and $\tan(q_i)$, respectively, and I is the identity matrix. Note that there is a Euler angle (roll (q_4), pitch (q_5), yaw (q_6)) singularity in J_2 when pitch angle is an odd multiple of 90° . Generally, the pitch angle in practical operation is restricted between less than $\pm 90^\circ$. However, if we need to avoid singularity altogether, unit quaternions can be used to represent orientation.

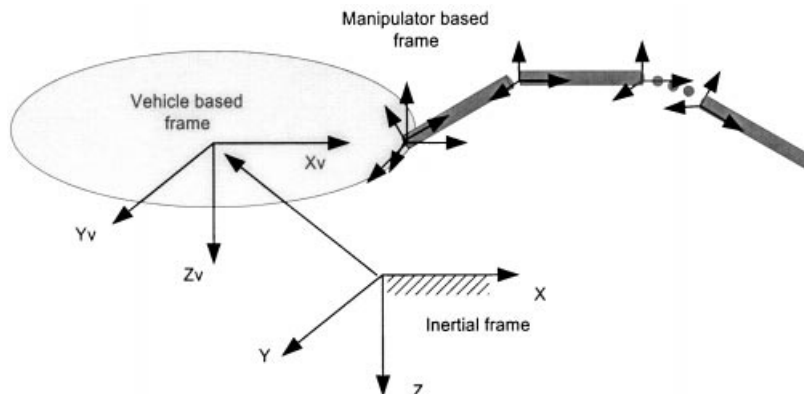


Fig. 2. Coordinate frames for a UVMS.

3.3 Thruster model

The AUV of the UVMS is propelled by hydrodynamic thrusters and the robot manipulator of the UVMS is driven by DC motors. While the dynamics of the actuators of the manipulator is not critical, Yoerger et al.¹⁹ pointed out that the system dynamics of an underwater vehicle can be greatly influenced by the dynamics of the thrusters, and neglecting this dynamics may result in a limited bandwidth controller with limit cycle instability. There are several dynamic models for marine thrusters that can reliably account for thruster dynamics. We include thruster dynamics in our control system to make the dynamic model, of the UVMS more realistic where the AUV is modeled as the slower dynamic system than the manipulator because of the thruster dynamics.

In order to relate the generalized force vector τ with the individual thruster/actuator forces/torques, let us consider a UVMS that has p thrusters and n actuators. Generally there are more than 6 thrusters in an AUV. Therefore, we consider $p \geq 6$. In such a case, we can write

$$\tau_b = EF_{td} \quad (9)$$

where E is a $(6+n) \times (p+n)$ thruster-actuator configuration matrix, and $F_{td} = [F_{td,v} \ F_{td,m}]$, in which $F_{td,v}$ is the vector of the thruster forces and $F_{td,m}$ is the vector of the actuator torques of the manipulator.

The matrix E captures the geometry of the UVMS and its thruster and actuator locations to transform the individual thruster force and actuator torques into generalized forces in the body-fixed frame of the AUV.

Thus the desired thruster force and motor torque distribution is obtained as

$$F_{td} = E^+ \tau \quad (10)$$

where $E^+ = E^T(EE^T)^{-1}$ is the pseudoinverse of E when $p > 6$ and $E^+ = E^{-1}$ when $p = 6$.

The desired thruster force distribution obtained from Equation (10) is required to achieve the desired motion of the AUV of the UVMS. This desired thruster force serves as the input to a thruster dynamic model. In this work we use the model proposed by Healey et al.,²⁰ which included a four-quadrant mapping of the lifts and drag forces of the propeller blades and was coupled with the motor and fluid system dynamics. This model is given by the following equations:

$$\Omega_r = \alpha_2^{-0.5} \text{sign}(F_{td,v}) |F_{td,v}|^{0.5} \quad (11)$$

$$i_m = K_t^{-1} \alpha_1 F_{td,v} + K_f^{-1} K_{fb} (\Omega - \Omega_r) \quad (12)$$

$$\dot{\Omega} = I^{-1} [K_t i_m - K_f \Omega - \mathfrak{S}] \quad (13)$$

where Ω and Ω_r are the actual and the desired/reference propeller angular velocity, respectively, and i_m is the motor current. The other parameters are: $\alpha_2 = \rho A r^2 \eta^2 \tan^2(\gamma)$, where ρ is the density of the water, r is the radius of the propeller, A is the thruster duct area, η is the propeller efficiency and γ is average pitch of the propeller blade, α_1 is an experimentally determined constant, K_t is the motor torque constant, K_f is the motor viscous friction constant, K_{fb} is the motor feedback gain, and \mathfrak{S} is the propeller shaft torque.

The propeller torque and the axial thrust are related to the blade lift, L and the drag, D as follows:

$$\mathfrak{S} = 0.7rL \sin \theta + D \cos \theta \quad (14)$$

$$F_{t,act} = L \cos \theta - D \sin \theta \quad (15)$$

where $F_{t,act}$ is the propeller shaft thrust, $\theta = \gamma - \alpha$, α is the angle of attack.

This actual thruster force, $F_{t,act}$, will be produced by the UVMS thruster considering the thruster dynamics.

4. DESIGN OF A UNIFIED FORCE CONTROLLER

In this section, we design the proposed unified force controller for a general UVMS. We describe how to design the impedance controller, the hybrid position/force controller and how to combine them using fuzzy switching. We also present how to include the thruster dynamics in the controller design.

4.1 Impedance Controller Design

The desired impedance for a linear system can be specified as

$$sZ(s) = Ps^2 + B_d s + K \quad (16)$$

where Z is the mechanical impedance of the system, P is an inertia gain matrix, B_d is a damping gain matrix, K is a stiffness gain matrix and s is a Laplace variable.

Impedance control has been implemented in many forms.¹⁴ Generally, there are two types of impedance control approaches, one is position-based and the other is torque-based.²¹ The former control scheme uses the force feedback sensed via force/torque sensor mounted at the wrist of the manipulator to adjust the position commands for the inner position loop controller by an impedance function, which can be expressed as

$$F_e = P\ddot{X}_a + B_d \dot{X}_a + KX_a \quad (17)$$

where P , B_d , K are inertia, damping and stiffness matrices, respectively. X_a is the position adjustment vector and F_e is the contact force.

The position-based impedance control relies on accurate position control of the system. The torque-based scheme, on the other hand, can provide small stiffness and damping, which is suitable for applications with small loads and slow motion. The stability issues of these two impedance control methods were discussed in detail in reference [21].

The motion of the end-effector of a UVMS is usually slow and without heavy loads. So the torque-based impedance method is suitable to meet the requirement and will be used in this paper. However, in such a case, the dynamic equation (8), which is expressed in the vehicle-fixed frame must be transformed into the inertial frame because torque-based impedance controller is normally designed in the inertial frame. Equation (8) can be rewritten in terms of the generalized coordinates:

$$M(q)\ddot{q} + C(q, \dot{q})\dot{q} + D(q, \dot{q})\dot{q} + G(q) = \tau - \tau_e \quad (18)$$

where

$$\begin{aligned} M(q) &= B^{-T} M_b(q_m) B^{-1} \\ C(q, w) &= B^{-T} [C_b(q_m, w) - M_b(q_m) B^{-1} \dot{B}] B^{-1} \\ D(q, w) &= B^{-T} D_b(q_m, w) B^{-1} \\ G(q) &= B^{-T} G_b(q) \\ \tau &= B \tau_b \\ \tau_e &\text{ is a } (6 \times n) \times 1 \text{ vector of external disturbance joint torque.} \end{aligned}$$

For simplicity, we denote

$$\zeta(q, w) = C(q, w)\dot{q} + D(q, w)\dot{q} + G(q) \quad (19)$$

so that (18) can be rewritten as

$$M(q)\ddot{q} + \zeta(q, \dot{q}) = \tau - \tau_e \quad (20)$$

The target impedance relationship between the end-effector and the environment can be expressed in the task-space:

$$F_e = P\ddot{E} + B_d\dot{E} + KE \quad (21)$$

where P , B_d and K are symmetric, positive-definite desired inertia, damping, and stiffness gain matrices, respectively. $E = X_d - X$, where X_d is the reference end-effector trajectory.

The relationship between the joint velocity and the Cartesian space velocity is

$$\dot{X} = J\dot{q} \quad (22)$$

where J is the Jacobian matrix with respect to the inertial frame. \dot{X} is the vector of task-space velocity, and \dot{q} is the $(6+n) \times 1$ vectors of the joint-space velocities.

By differentiating (22), we get the task-space and joint-space acceleration relationship:

$$\ddot{X} = J\ddot{q} + \dot{J}\dot{q} \quad (23)$$

The complete joint-space solution can be written as follows

$$\ddot{q} = J^+(\ddot{X} - \dot{J}\dot{q}) + (I - J^+J)\ddot{\phi} \quad (24)$$

where $J^+ = J^T(JJ^T)^{-1}$ is called Moore-Penrose pseudoinverse. $(I - J^+J)\ddot{\phi}$ is the null-space vector of J . I is the identity matrix and $\ddot{\phi}$ is an arbitrary vector which can be utilized to optimize various performance criteria. In this paper we do not include the null-space part of the solution in the controller design.

Substituting (24) (without null-space vector) into (20) yields

$$M(q)J^+(\ddot{X} - \dot{J}\dot{q}) + \zeta(q, \dot{q}) = \tau - \tau_e \quad (25)$$

The relationship between the actuator forces and joint torques is

$$\tau = J^T F \quad (26)$$

The dynamic equation of the UVMS is now given by

$$\tilde{J}^+ M J^+ (\ddot{X} - \dot{J}\dot{q}) + \tilde{J}^+ (\zeta) = F - F_e \quad (27)$$

where $\tilde{J} = J^T$.

Finally, we can write the vehicle and manipulator dynamic equation model in the Cartesian space:

$$\tilde{M}\ddot{X} + \tilde{\zeta} = F - F_e \quad (28)$$

where $\tilde{M} = \tilde{J}^+ M J^+$, $\tilde{\zeta} = \tilde{J}^+ \zeta - \tilde{M} \dot{J} J^+ \dot{X}$.

We now design the torque-based impedance control scheme based on the UVMS model expressed in the Cartesian space. The control law is given by

$$F = \hat{M}U + \hat{\zeta} + F_e \quad (29)$$

where \hat{M} , $\hat{\zeta}$ are estimates of $\tilde{M}\tilde{\zeta}$ and F_e is the exerted force on the environment, and

$$U = \ddot{X}_d + P^{-1}[B_d(\dot{X}_d - \dot{X}) + K(X_d - X) - F_e] \quad (30)$$

Substituting (28) into (29), we get

$$F = \hat{M}\{\ddot{X}_d + P^{-1}[B_d(\dot{X}_d - \dot{X}) + K(X_d - X) - F_e]\} + \hat{\zeta} + F_e \quad (31)$$

From (28)

$$F = \tilde{M}\ddot{X} + \tilde{\zeta} + F_e \quad (32)$$

From (31) and (32)

$$\begin{aligned} \hat{M}\{\ddot{X}_d + P^{-1}[B_d(\dot{X}_d - \dot{X}) + K(X_d - X) - F_e]\} \\ + \hat{\zeta} + F_e = (\tilde{M} - \hat{M})\ddot{X} + \tilde{\zeta} + F_e \end{aligned} \quad (33)$$

We set $E = X_d - X$, $\Delta\tilde{M} = \tilde{M} - \hat{M}$, $\Delta\tilde{\zeta} = \tilde{\zeta} - \hat{\zeta}$, to obtain

$$\ddot{E} + P^{-1}(B_d\dot{E} + KE - F_e) = \hat{M}^{-1}(\Delta\tilde{M}\ddot{X} + \Delta\tilde{\zeta}) \quad (34)$$

If $\Delta\tilde{M} = \Delta\tilde{\zeta} = 0$, the closed-loop of the underwater vehicle and manipulator system satisfies the target impedance relationships (21).

4.2 Hybrid position/force controller design

Many advanced control algorithms have been developed for the position and force subsystem of the hybrid control. In this paper, we use a simple PD controller for position control and a PID controller for force control. The control law can be formed as a combination of position and force control:

$$F = [I - S]F_p + [S]F_f + \hat{\zeta} + F_e \quad (35)$$

where I is the identity matrix and S is the compliance selection matrix. F_p is the output of the position controller and F_f is the output of the force controller. $\hat{\zeta}$ is the estimation of Coriolis/centripetal and gravity vector. F_e is the contact force between the end-effector and the environment. If $\hat{\zeta} \approx \tilde{\zeta}$, we combine equation (28) (35)

$$\tilde{M}\ddot{X} = [I - S]F_p + [S]F_f \quad (36)$$

This is a closed loop dynamic model, which has the explicit relationship between position input and torque output.

For the position control law, consider a PD controller with acceleration feed-forward term

$$F_p = \hat{M}(\ddot{X}_d + K_{pv}\Delta\dot{X} + K_{pp}\Delta X) \quad (37)$$

where $\Delta X = X_d - X$. The position error equation becomes

$$\Delta\ddot{X} + K_{pv}\Delta\dot{X} + K_{pp}\Delta X = 0 \quad (38)$$

Similarly a PID control law can be used for force control part.

$$F_f = \hat{M}(\ddot{F}_d + K_{fp}\Delta F + K_{fi} \int \Delta F dt + K_{fv}\Delta \dot{F}) \quad (39)$$

sented as the ratio of the contact force and the desired force F_e/F_d , and the velocity of the end-effector v_e in the normal direction to the surface of the environment. The output of the fuzzy switching module is the desired weight. The membership functions of F_e/F_d are specified as *FS* (small), *FM* (medium) and *FL* (large). The membership functions of v_e are defined as *VS* (slow) and *VF* (fast). The membership functions of the switching weight are defined as *WS* (weight small), *WM* (weight medium) and *WL* (weight large) as shown in Fig. 4.

The fuzzy switching rules can be expressed as

IF F_e/F_d is F_i **AND** v_e is V_j **THEN** weight is W_k ;

where F_i is the force feedback set, $F_i \in \{FS, FM, FL\}$; V_j is velocity set, $V_j \in \{VS, VF\}$; W_k is switching weight set, $W_k \in \{WS, WM, WL\}$. The relationship between the two fuzzy inputs and one fuzzy output can be represented by a two-dimensional surface as shown in Fig. 5.

We have used three fuzzy rules to combine the output of impedance control with that of the hybrid position/force control. They are

- ⇨ **IF** F_e/F_d is *FS* **AND** v_e is *VF* **THEN** weight is *WL*;
- ⇨ **IF** F_e/F_d is *FM* **THEN** weight is *WM*;
- ⇨ **IF** F_e/F_d is *FL* **AND** v_e is *VS* **THEN** weight is *WS*.

5. RESULTS AND DISCUSSION

5.1 Simulation Model

Currently there is no autonomous UVMS available for us to implement the proposed controller. Therefore we have performed extensive computer simulations to investigate the effectiveness of the proposed unified force control approach. The UVMS considered for the simulations consisted of a 6 DOF vehicle and a 3 DOF robotic manipulator. The ellipsoidal vehicle is 1.0 m long, 0.5 m high, 0.5 m wide and 530.0 kg in weight. The links of the manipulator are cylindrical in shape having the following dimensions: length=0.5 m each, radius of link 1=0.05 m, radius of link 2=0.04 m and radius of link 3=0.035 m. The masses of links are: $m_1=10$ kg, $m_2=8$ kg and $m_3=5$ kg. The

drag coefficients for the vehicle are: linear drag coefficients for linear and rotational motions are 0 and 0.81; quadratic drag coefficients for linear and rotational motions are 1.05 and 1.0, and quadratic drag coefficient for the manipulator is 1.1. For this unified force control scheme, we have chosen a circular trajectory (radius 0.1 m) in the inertial frame, i.e., in the task-space with zero initial velocity and acceleration. We have considered a solid environment like a vertical wall at a distance of $x=1.7771$ m. A schematic diagram of the set-up is given in Fig. 6. For simplicity, we do not consider the friction along the surface of the environment.

5.2 Case study

We have conducted several case studies with this system to test the performance of the proposed force controller under different working conditions, such as with different stiffness of the environment, with force sensor noise, with the motion of the environment, and without complete compensation for the system dynamics. A half-circular trajectory was designed to test the performance of the proposed controller to realize unconstrained motion, smooth contact and force trajectory tracking. As shown in Fig. 7, the end-effector moves along the circular trajectory toward the environment (from A to B). Then it makes a smooth contact during the transient phase by the fuzzy switching law. The surface is compressed because of the application of force and the contact force point B moves to point B'. The end-effector of the manipulator is required to follow the desired force trajectory (150N) while sliding down along the environment surface (from B' to C') after it encounters the surface. Then it leaves the wall (from C' to C) and moves back to the free motion trajectory (from C to D). It should be noted that the surface is compressed to generate the desired contact force. The dashed curve indicates the desired circular motion trajectory if the surface were not present.

5.3.1 Case I: Surfaces with different stiffness. The objective of this simulation is to test the performance of the unified force controller during transient phase when contacting with environment with different stiffness. We select two environment stiffness values ($K_e=1e4$ & $1e5$ N/m) for this case. As shown in Fig. 8 and Fig. 9, the proposed force

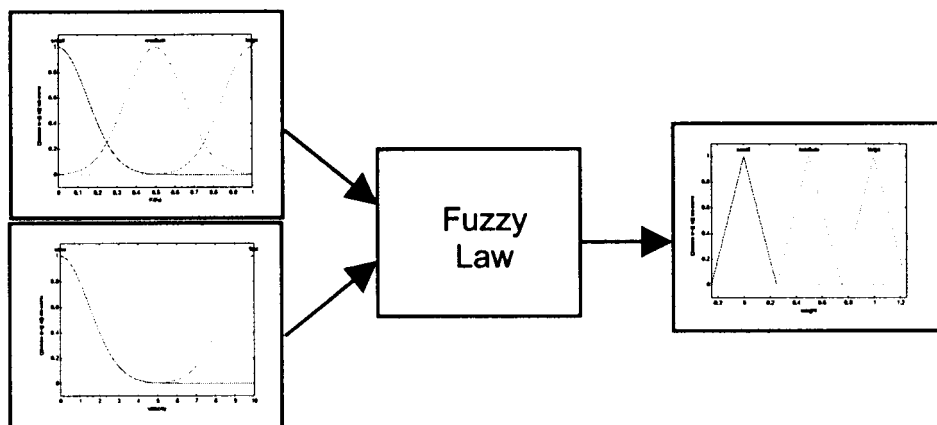


Fig. 4. Fuzzy switching law.

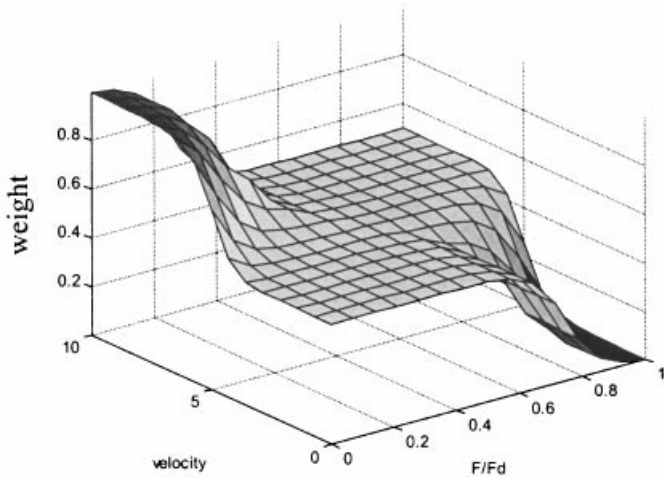


Fig. 5. Fuzzy input/output mapping surface.

control scheme follows the desired force trajectory well during the constrained motion phase. For high stiffness environment ($K_e=1e5$ N/m), the overshoot of the force response is slightly higher than that of low stiffness environment ($K_e=1e4$ N/m). However, we achieve stable contact in both cases. Figure 10 shows that the position errors are very small in the Y and Z directions. The relatively large error in the X direction in the middle of the curve is due to the presence of the wall inside the desired motion trajectory. We can also see the weight change between 0 and 1 by the fuzzy switching law based on the contact force and velocity of the end-effector.

5.3.2 Case II: Noisy force feedback. We generally cannot obtain force feedback without noise for a real system. In this case study, we add sensor noise in the force feedback. For JR3 6 DOF force/moment sensor,²³ the noise level is 0.1% of the range.

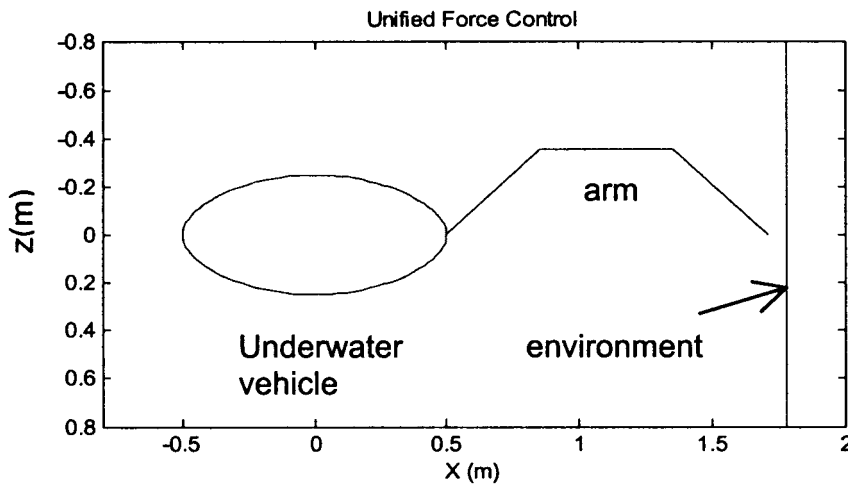


Fig. 6. Schematic diagram of the system set-up.

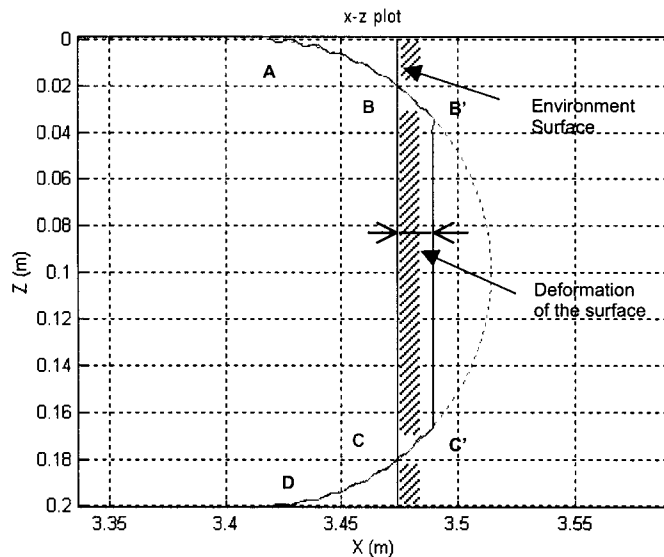


Fig. 7. End-effector trajectory.

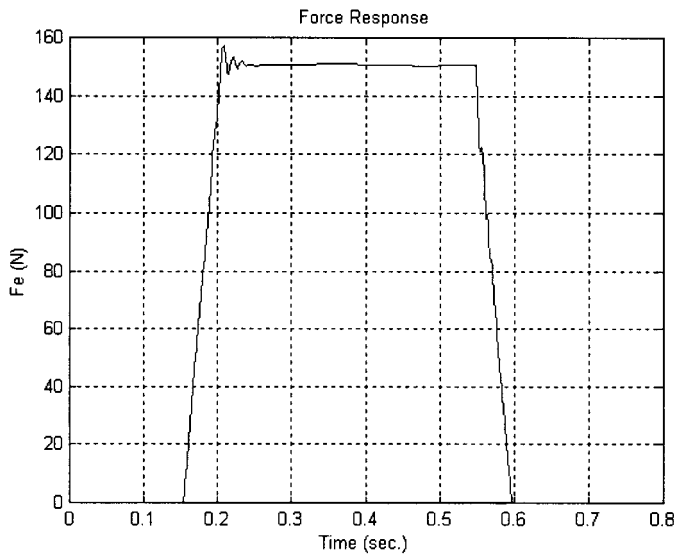


Fig. 8. Force response ($K_e = 1e4$ N/m).

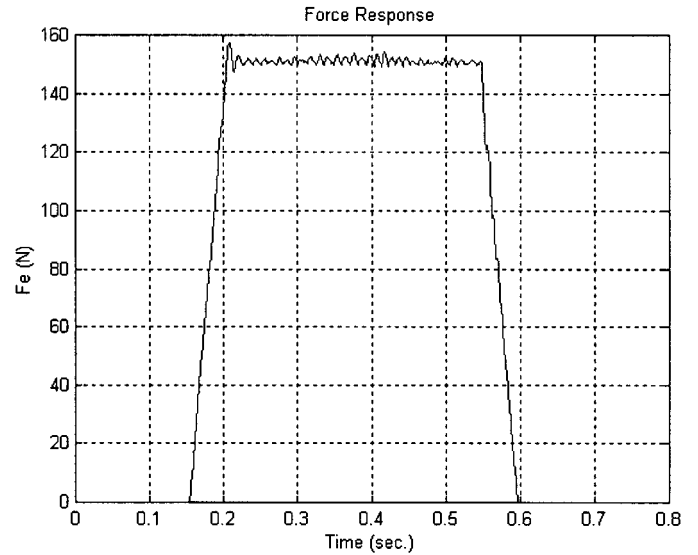


Fig. 11. Force response with force sensor noise ($K_e = 1e4$ N/m).

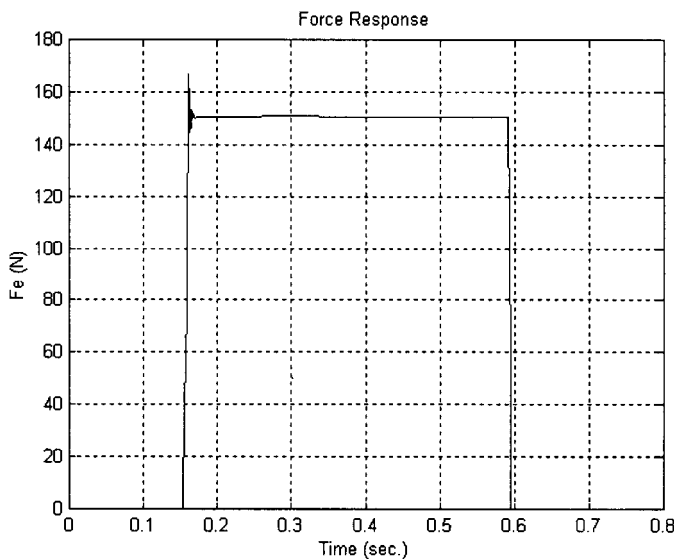


Fig. 9. Force response ($K_e = 1e5$ N/m).

Figure 8 and Fig. 11 present the force responses in the case with and without force sensor noise. It is observed that the proposed force control scheme can tolerate force sensor noise within a certain degree.

5.2.3 Case III: Contact with a moving surface.

Figures 12 and 13 show a special case. In this case, after the end-effector contacts with the wall, the wall begins to move with a speed in X direction ($V_e = 0.05$ m/s). Figure 12 gives the force response for this case. We can see the unified force control scheme can maintain the control force well even when the wall is moving. Figure 13 gives the actual end-effector trajectory. Figure 14 provides the movement of the UVMS during this test case. It is clearly seen that the contact force has little effect on the vehicle. This is mainly due to the smooth contact force and the relatively large vehicle mass. In this simulation, we have not incorporated the null-space solution of Equation (22). It can be utilized to satisfy various performance criteria such as singularity

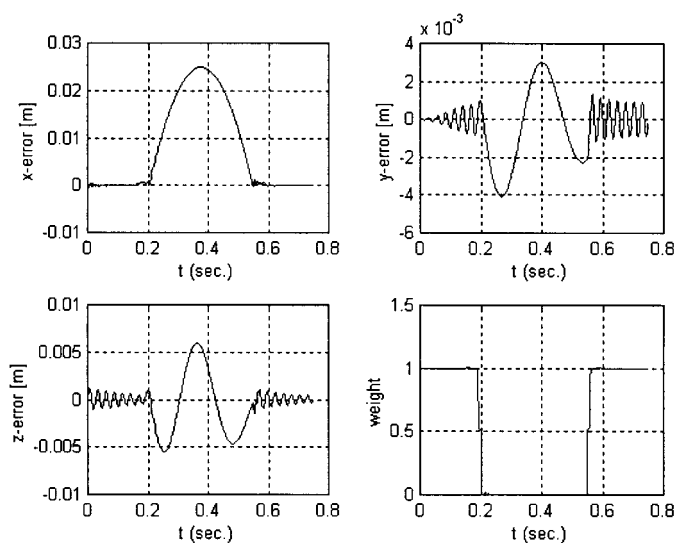


Fig. 10. Position errors and weight response.

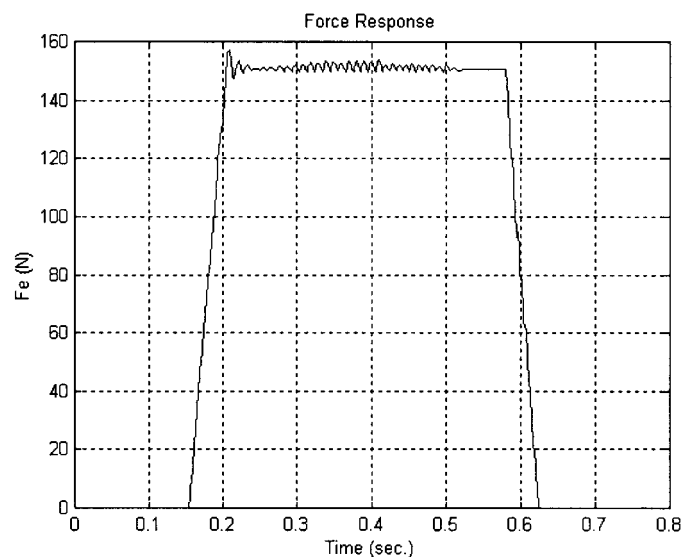


Fig. 12. Force response (with wall movement).

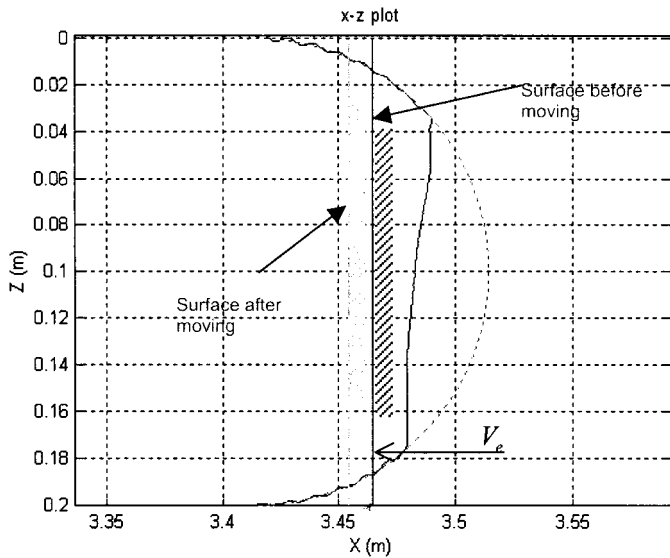


Fig. 13. End-effector trajectory (with wall movement).

avoidance, joint limit avoidance, obstacle avoidance, energy minimization and various other criteria.

5.2.4 Case IV: Partial dynamic compensation. As we have discussed in Section 3, it is difficult to obtain an accurate model of the UVMS. In this case, we assume the $\Delta\tilde{M} \neq 0$. Here we set $\hat{M} = 0.9\tilde{M}$. The corresponding contact force is shown in Fig. 15. It is indicated that the new force control scheme has a good degree of robustness, which is crucial for UVMS.

6. CONCLUSIONS

We have investigated a unified force control approach for an underwater vehicle-manipulator system that allows the system to interact with the environment in a smooth and stable manner. The desired force trajectory can be realized using the same controller by fuzzy switching laws. This approach combines two well-known control approaches namely, impedance control and hybrid position/force con-

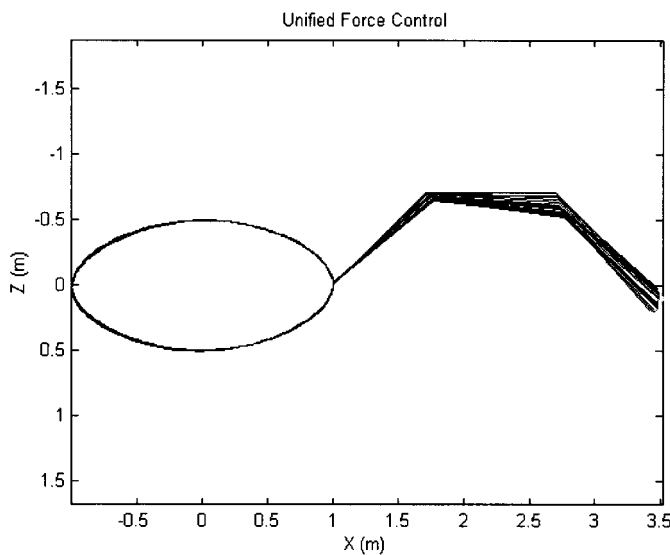


Fig. 14. UVMS movement during force control.

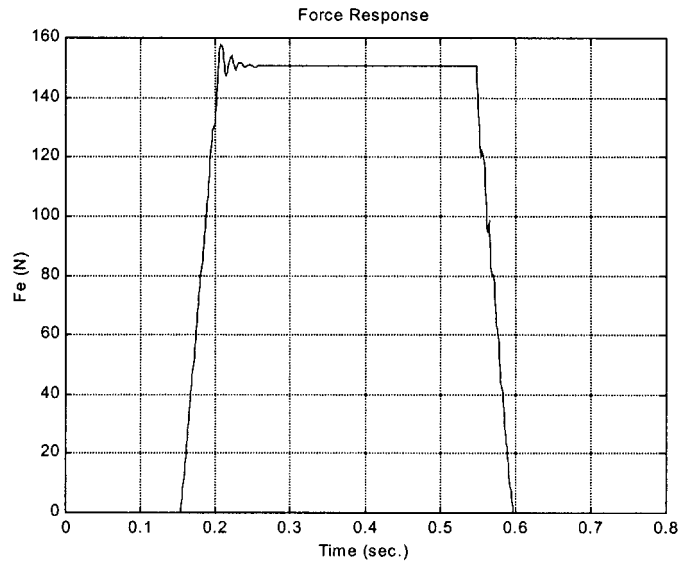


Fig. 15. Force response when $\Delta\tilde{M} \neq 0$

trol, in such a way that unconstrained motion, contact transition and force trajectory tracking can be achieved by a single controller. One advantage of the controller is that it can track a force trajectory without needing information about the environment. Thus this controller will be potentially useful for underwater tasks where environmental information is generally not available. We have designed the controller based on a dynamic model of the UVMS that considers major hydrodynamic effects. Since we do not focus on hydrodynamics, we have chosen shapes for our UVMS for simulation in such a way that analytical expressions for various hydrodynamic parameters are available in the literature. However, it should be noted that the theoretical framework is completely general and does not require that the geometry of the UVMS be simple. This model is further improved by including the dynamic model of the thrusters. We have tested the proposed controller by extensive computer simulations and the results appear to be promising.

This proposed controller is not without its shortcomings and needs to be improved in future. For a real UVMS, it is difficult to get an accurate model of the system, especially for the hydrodynamic part. This is not a limitation of our work alone, most autonomous control of a UVMS will need to have the knowledge of these parameters. Adaptive and learning control methods will be employed in future to compensate for the inaccuracy of the system model.^{24,25} Neural Network-based techniques can be used to dynamically adjust both the membership function and the fuzzy rules based on the system information. The fuzzy logic itself can also be made more sophisticated to improve the switching performance. We require derivative of the force for the force control subsystem of the hybrid position/force controller, which introduces noise in the system. Although the controller is shown to work well with a limited noise, noise reduction techniques must be employed if the performance falls below the acceptable limit. Finally, the proposed force control strategy will need to be further verified by experiments on a UVMS when such a system becomes available in future.

Acknowledgements

This study was sponsored in part by the NSF under grant BES97-01614 and the ONR under grant N00014-97-1-0961.

References

1. J. Yuh, *Underwater Robotic Vehicles: Design and Control* (TSI Press Series, Albuquerque, NM, 1995).
2. S. McMillan, D.E. Orin & R.B. McGhee, "Efficient Dynamic Simulation of an Underwater Vehicle with a Robotic Manipulator", *IEEE Transactions on Systems, Man, and Cybernetics* **25**, No. 8, 1194–1206 (August, 1995).
3. M.W. Dunnigan & G.T. Russell, "Evaluation and Reduction of the Dynamic Coupling Between a Manipulator and an Underwater Vehicle", *IEEE Journal of Oceanic Engineering* **23**, No. 3, 260–273 (July, 1998).
4. N. Sarkar, J. Yuh & T. Podder, "Adaptive Control of Underwater Vehicle-Manipulator Systems Subject to Joint Limits", *Proceedings of the IEEE/RSJ International Conference on Intelligent Robots and Systems (IROS)* (1999) pp. 142–147.
5. N. Sarkar and T. Podder, "Motion Coordination of Underwater Vehicle-Manipulator Systems Subject to Drag Optimization", *IEEE International Conference on Robotics and Automation*, Detroit, Michigan (May 10–15, 1999) pp. 387–392.
6. M.W. Dunnigan, D.M. Lane, A.C. Clegg and I. Edwards, "Hybrid Position/Force Control of a Hydraulic Underwater Manipulator", *IEE Proceedings Control Theory and Application* **143**, No. 2, 145–151 (March, 1996).
7. H. Kajita & K. Kosuge, "Force Control of Robot Floating on the Water Utilizing Vehicle Restoring Force", *Proceedings of the 1997 IEEE/RSJ International Conference on Intelligent Robot and Systems* (1997) **Vol. 1**, pp. 162–167.
8. L. Lapierre, P. Fraisse & N. K. M'sirdi, "Hybrid Position/Force Control of a ROV with a Manipulator", *OCEAN '98 Conference Proceedings* (1998) **Vol. 2**, pp. 931–935.
9. G. Antonelli, N. Sarkar and S. Chiaverini, "An external force control scheme for underwater vehicle-manipulator systems", *Proceedings of the IEEE International Conference on Decision and Control* (1999), **Vol. 3**, pp. 2975–2980.
10. Y. Cui, T. Podder & N. Sarkar, "Impedance Control of Underwater Vehicle-Manipulator Systems (UVMS)", *Proceedings of the IEEE/RSJ International Conference on Intelligent Robots and Systems (IROS)* (1999) **Vol. 1**, pp. 148–153.
11. R. Anderson & M.W. Spong, "Hybrid Impedance Control of Robotic Manipulators", *IEEE Journal of Robotics and Automatics*, **4**(5), 549–556 (1988).
12. H. Seraji & R. Colbaugh, "Force Tracking in Impedance Control", *IEEE International Conference on Robotics and Automation*, Atlanta (2–6 May, 1993) pp. 499–506.
13. M. Shibata, T. Murakami & K. Ohnishi, "A Unified Approach to Position and Force Control by Fuzzy Logic", *IEEE Transactions on Industrial Electronics* **43**, No. 1, 81–87 (1996).
14. D.E. Whitney, "Historical Perspective and State of the Art in Robot Force Control", *IEEE Proceedings of the International Conference on Robotics and Automation* (1985) pp. 262–268.
15. G. Zeng and A. Hemami, "Overview of Robot Force Control", *Robotica* **15**, Part 5, 473–482 (September–October, 1997).
16. M.H. Raibert and J.J. Craig, "Hybrid Position/Force Control of Manipulators", *ASME Journal of Dynamic Systems, Measurement, and Control* **102**, 126–133 (June, 1981).
17. N. Hogan, "Impedance control: An approach to manipulation, parts I–III", *ASME Journal of Dynamic Systems, Measurement, and Control* **107**, No. 1, 1–24 (1985).
18. L. Meirovitch, *Methods of Analytical Dynamics* (McGraw-Hill Book Co., New York, 1970).
19. D.R. Yoerger & J.J.E. Slotine, "Robust trajectory control of underwater vehicles", *IEEE Journal of Oceanic Engineering* **10**, No. 4, 462–470 (1990).
20. A.J. Healy, S.M. Rock, S. Cody, D. Miles and J.P. Brown, "Toward an improved understanding of thruster dynamics for underwater vehicles", *IEEE Journal of Oceanic Engineering* **20**, No. 4, 354–361 (1995).
21. D.A. Lawrence, "Impedance Control Stability Properties in Common Implementations", *IEEE International Conference on Robotics and Automation* (April, 1988) pp. 1185–1190.
22. D. Driankov, H. Hellendoorn & M. Reinfrank, *An Introduction to Fuzzy Control* (Springer-Verlag, Berlin Heidelberg, 1993).
23. *JR3 Software and Installation Manual* (JR3 Inc., 1994).
24. S. Jung & T.C. Hsia, "Neural Network Impedance Force Control of Robot Manipulator", *IEEE Transactions on Industrial Electronics* **45**, No. 3, 451–461 (June, 1998).
25. R. Colbaugh, H. Seraji & K. Glass, "Direct Adaptive Impedance Control of Robot Manipulators", *Journal Robotic Systems* **10**, No. 2, 217–248 (1993).